Hindawi
Shock and Vibration
Volume 2018, Article ID 3953259, 16 pages
https://doi.org/10.1155/2018/3953259

Research Article

Study on the Failure of the Bolted Flange Connection Structure between Stages of Missiles (Rockets) under Transverse Impact Load

Tonghui Tian,[1] **Jiehong Yuan**,[1] **Daokui Li**,[1] **Qingwen Wang**,[1] **and Baisheng Chen**[2]

[1]*College of Aerospace Science and Engineering, National University of Defense Technology, Changsha 410073, China*
[2]*College of Civil Engineering, Hunan University, Yuelu Mountain, Changsha 410082, China*

Correspondence should be addressed to Tonghui Tian; tiantonghui16@nudt.edu.cn

Received 5 August 2018; Revised 7 October 2018; Accepted 22 October 2018; Published 2 December 2018

Academic Editor: Itzhak Green

Based on the bolted flange connection structure between stages of the missiles, four experimental specimens are simplified and manufactured, and the transverse impact failure experiments of the drop hammer are designed and carried out in this study. During the experiments, a new signal sensor is designed to collect the data of the bolts force, and the response data such as the bolts force, the slotted displacement of the connecting interface, and the impact force are collected in the loading process. The sequential failure mechanism of the structure under transverse impact load is analyzed and demonstrated according to the experimental results and the measured data. Additionally, a finite element model to simulate the failure process of the connection structure has been established, and the precision of the model has been verified and validated according to the experimental results. Moreover, the comparison between the results of the experiments and the simulation shows that the precision of this model is reliable in the engineering.

1. Introduction

The bolted flange connection structure is an important part of the missile structure as the separated connecting structure between stages. Due to strong nonlinear characteristics of the structure [1], the geometric continuity of the missile body is destroyed, and some problems such as excessive local deformation and stress concentration are easy to occur in the course of loading [2]. Thus, the connection structure is a weak component that is prone to fail, which weakens the load bearing capacity of the whole structure [3]. In the course of launching and flying at the high speed, the rocket or missile may be subjected to transient abnormal loads with the extremely unstable amplitude and location. For example, during the effluent process of a submarine-launched missile, a pressure pulse whose amplitude exceeds 10 MPa will be formed when a large number of bubbles on the surface of the missile collapse in millisecond after contacting with the atmosphere, which may result in the failure of the connection structure between stages [4]. Due to the complex mechanical properties [5] of the connection structure, such as the nonlinear problems of the slip between contacting interfaces [6] and geometric discontinuity [7], theoretical analysis and solutions are difficult to be established [8]. As a result, it is of great engineering and theoretical significance to research the failure mechanism of the connection structure under transient impact load by the experimental or the finite element method.

Most of the experimental concerns about the bolted flange connection structure have been focused on the vibration characteristics under dynamic load and the load bearing characteristics under static load. Besides, the failure experiment under impact load has not been found carried out and investigated. In 2013, Van-Long et al. designed and carried out quasistatic load failure experiments concerning the bolted connection structure under axial monotonic and cyclic loading. The mechanical properties and the behavior of these connections for low cycle and high cycle fatigue have been obtained and characterized [9]. Prinz et al. carried

out horizontal quasistatic loading experiments on bolted beam-column structures, the numerical simulation model is established according to this structure, and a reasonably accurate of the finite element model with shell elements and nonlinear springs for the loading response is verified [10]. Guo et al. proposed a typical configuration of the bolted flange joint and investigated the response of vibration and dissipation of the joint under a series of impact loading with the simulation model, validated by a revised SHPB (Split Hopkinson pressure bar) experiment [11]. Consequently, the researcher's attention has been attracted in the experimental study on the typical bolted connection structure, and more failure experiment under different and complicated loading condition corresponding to different application background of these structures should be designed and implemented as a reference for the engineering application.

Some of the existing research studies of the bolted flange connection structure used by the finite element method simplified the connection structure as rigid connection which guarantees a higher computational efficiency [12], to calculate and analyze its response mechanism under transient impact load. In 2011, Luan et al. [13] and Lu et al. [14] investigated the nonlinear characteristic of the different tensile and compressive axial stiffness on the connection structure and established a simplified finite element model introducing the modified spring with nonlinear stiffness into the connecting interfaces which can reflect the dynamic response mechanism to a certain extent, yet the failure mode of the connection structure under transient dynamic load has not been considered in the proposed research. Simultaneously, with the development of computing power of the computer, the solid model of the bolt in simulation has been researched more and more to improve the degree of accuracy of the simulation. In 2000, Schaumann and Seidel present failure analysis results from detailed nonlinear FE calculation of bolted steel ring flange connections, and bearing capacity of the structure under quasistatic load has been predicted, but the failure criterion of the structure is plastic deformation, and the fracture failure mode of the bolts is not demonstrated in the research [15]. Abid and Nash have investigated the sealing property and tightening strategies for gasket flanged with bolted joint used by a solid FEM [16, 17]. In 2016, Bartlomiej and Witold established a finite element model through applying a multilevel substructuring approach and a reduction of DOFs using the static condensation method, and the mechanical behavior of the complex structure composed of tubular beams and bolted connections has been investigated [18]. However, the concern of these research studies is focused on the precision of the simulation on the mechanics parameters, stress analysis, and the load bearing capacity under quasistatic load of the bolted flange connection structure. Therefore, the simulation objective of the bolt fracture using the solid bolt model under different loading conditions should be considered into the further research schedule.

In the current work, the impact failure experiments of the bolted flange connection structure were designed and carried out, and the results of sequential failure have also been realized. A set of key data has been collected, and the failure mechanism of the connection structure under transient impact load has been analyzed and investigated. Additionally, a finite element model to simulate the failure process of the structure has been established corresponding to the experimental bolted flange connection structure with a solid bolt model, and the precision of the model has been verified and investigated in accordance with the measured data in the experiments.

2. Experimental Program

2.1. Specimen Preparation. Based on the structural geometrical characteristics of the bolted flange connection structure between stages of missiles, four experimental specimens were designed and manufactured considering the factors of the same structure composition as the actual structure, the convenient size for research, and appropriate production costs. The structure of the experimental specimens is mainly composed of two levels of the fuselage column segment, bolts, shear pins and cushion blocks, assembled as shown in Figure 1, while the dimensioning labels of the specimen are presented in Figure 2.

Among them, the diameters of bolts used in experiments are 5 mm and 6 mm, respectively.

The cushion block thickness is 10 mm and the inner diameter is 6 mm, while the outer diameter is 18 mm.

The shear pin column segment diameter is 5 mm, the column segment length is 10 mm, and the cone segment length is 6 mm, while the cone taper is $\gamma = 6.8^{\circ}$.

The column segment wall thickness is 4 mm, the total height is $H = 350$ mm, the inner flange thickness is 10 mm, and the inner diameter and the outer diameter of the inner flange are $d_1 = 225$ mm and $d_2 = 295$ mm, respectively. The outward flange thickness is 10 mm and the inner diameter and the outer diameter of the outer flange are $D_1 = 287$ mm and $D_2 = 350$ mm, respectively.

There are 8 or 12 bolt holes and shear pin holes uniformly distributed on the internal flange in different specimens. The diameter of the distribution circle of the bolt group is 251 mm, the diameter of the bolt hole is 5 mm, 6 mm, or 10 mm, and the angle between bolt holes and shear pin holes is 6° in the distribution circle. The outward flange is uniformly distributed with 12 bolt holes, whose diameter is 4.5 mm.

The material used in the column segment and the cushion block is the aluminum alloy and the bolt is the grade 8.8 high strength bolt, while the material for shear pin is high strength alloy steel named 30CrMnSiNi2A. The total mass of the experimental specimen is 10.1 kg.

2.2. Experimental Scheme. The failure experiments of drop hammer were designed using the experimental specimens previously mentioned to fully reveal the failure mechanism of the bolted flange connection structure under impact load and to provide data support for numerical simulation. Different structural parameters such as the number of bolts, bolts distribution conditions, and the bolt diameter were considered and designed for comparison and analysis. The experimental grouping number and experimental

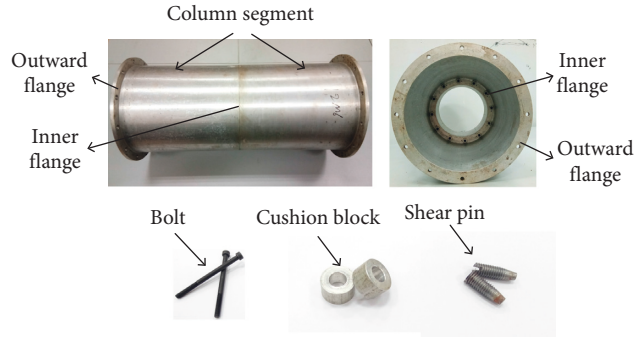

Figure 1: The experimental specimen.

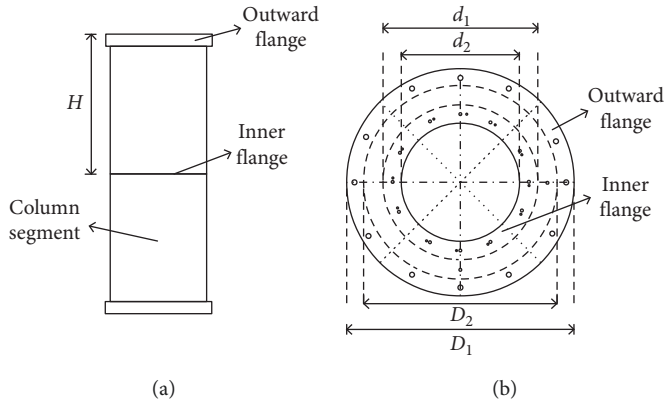

Figure 2: The diagram of dimensioning.

parameters are set up as presented in Table 1, while the distribution condition of the bolt group and the identifier number of bolts in experiments are shown in Figure 3, and the direction of arrows is the direction of impact loading.

The experimental specimen is larger in size and higher in strength, so the structure failure caused by drop hammer impact requires large instantaneous input energy. To prevent the column segment damage caused by the direct impact of the drop hammer, the impact load is transferred to the connection structure by installing the protective device at the free end. The experimental loading schemata are shown in Figure 4, the experimental specimen is installed in the pedestal horizontally, the bearing platform with the material of 45# iron is installed at the free end, and the impact load is transferred to the connection structure when impacting the bearing platform by the drop hammer.

The experiments were carried out on the high performance drop hammer experimental machine of the *Engineering Structure Protection Laboratory* in Hunan University. The diagram of the drop hammer experimental machine and the experimental tooling locale is shown in Figure 4.

It is difficult to directly apply strain gauges on the bolt screw and connect the electric wire for collecting the time history response signal of the bolt force for the coherent structural characteristics of the bolted flange. Thus, a special sensor is designed in Figure 5. The pressure signal of the sleeve can be collected through installing a bearing steel sleeve between the flange and the bolt nut and then applying the strain gauge on the external surface of the sleeve. The tension on the screw and the pressure on the sleeve are the relationship of the force and reaction force. Therefore, the response signal of the screw under tension can be obtained by conversion from the response signal of the sleeve under compression.

The failure process of the bolt group under impact load is extremely short, the time scale is in the order of milliseconds, and the demand of sampling frequency of the data signal is extremely high. The data measuring system is developed by NI Company in the United States used during the experiments and equipped with the high strain rate dynamic strain signal acquisition system that records (100 kHZ sampling frequency) the time history response data of strain. The acquisition position of the strain signal is the signal acquisition sensor of the bolt force and the middle points on the outer surface of the column segment. Meanwhile, the photoelectric velocity measuring device of the trigger mode was set up to collect the impact velocity of the hammer head, the force sensor was set up to record the impact force data, and the high-speed camera was set up to record the experimental process.

2.3. The Finite Element Model. In order to evaluate the safety of experimental tooling, determine whether the expected experimental results can be completed, and verify the

Table 1: The experimental grouping number and experimental parameters.

Experimental grouping identifier	Loading condition	Diameter of bolt hole	Number of bolt holes	Diameter of bolt	Number of bolts	Distribution condition of the bolt group
T-1	Transverse	M6	12	M6	8	Nonuniformly
T-2	Transverse	M5	12	M5	12	Uniformly
T-3	Transverse	M9	8	M6	8	Uniformly
T-4	Transverse	M10	8	M6	8	Uniformly

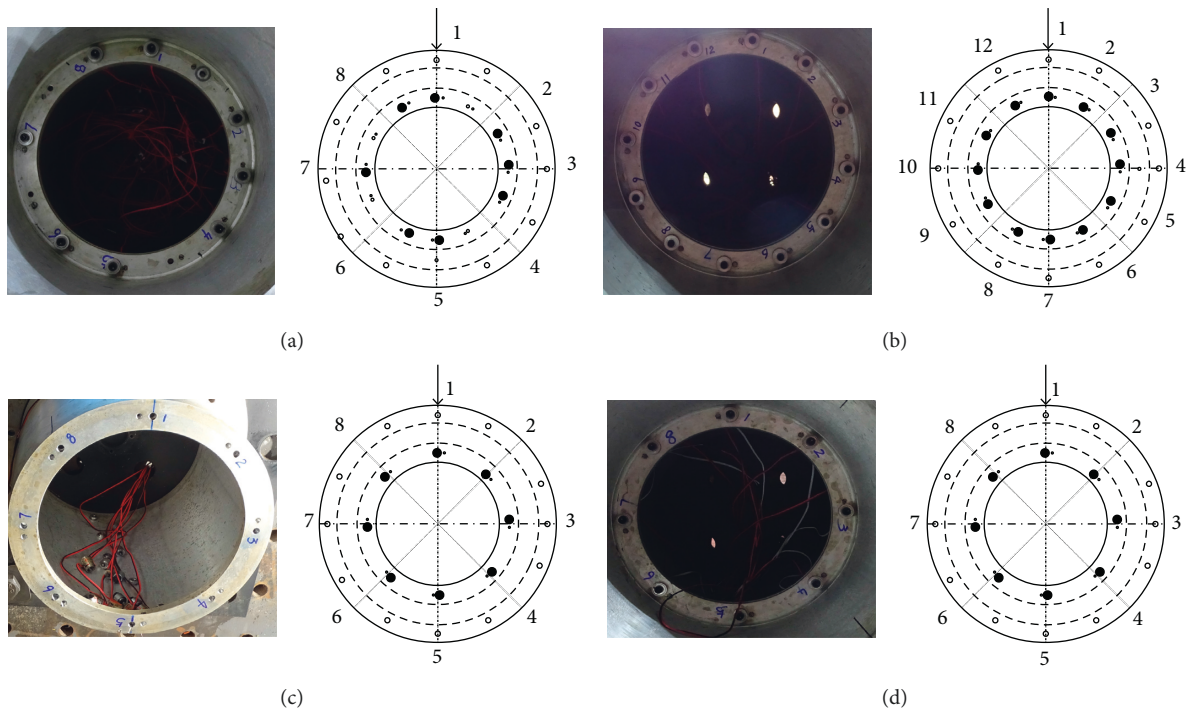

Figure 3: The distribution conditions and identifiers of the bolts. (a) T-1, (b) T-2, (c) T-3, and (d) T-4.

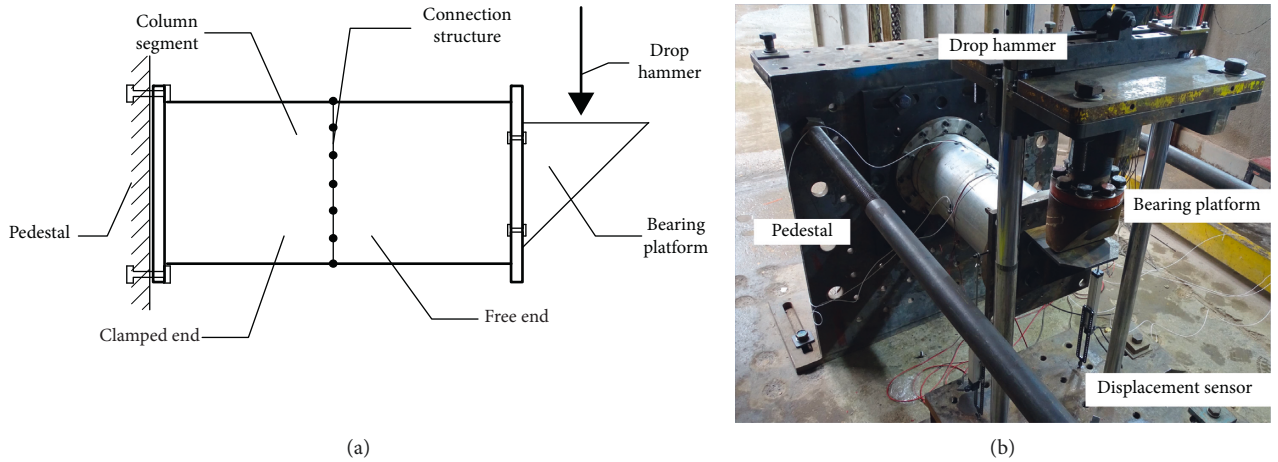

Figure 4: The schemata of the experimental loading and locale.

accuracy of the finite element model, ABAQUS, the commercial finite element software, is adopted to establish the finite element models consistent with the actual experiments. The finite element models and the calculation results can be found in Figure 6.

In the simulation model, the flange, bolts, bolt nuts, and cushion blocks are meshed using the hexahedral element with the reduced integral algorithm, and the column segment is meshed using the quadrilateral shell element with the reduced integral algorithm to improve the

Figure 5: The signal acquisition sensor of the bolts force.

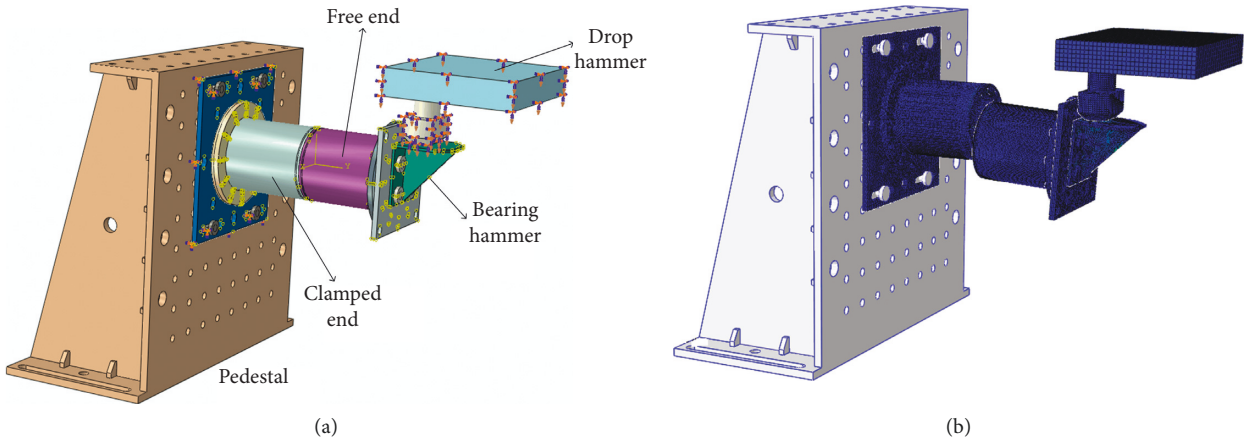

Figure 6: The finite element model. (a) Transverse impact experiment. (b) Calculation result.

calculation efficiency. And the test bed and pedestal are defined as the rigid body which has enough strength and small deformation.

The ABAQUS/Standard solver is used to apply pretightening force to bolts [19]. And it is difficult to establish the mesh of bolts with the thread for the complexity geometry of the bolt thread and the contact condition, and the model with complex mesh condition of the thread is hard to converge using the implicit algorithm, while it may even lead to calculation failure [20]. The mode of thread failure does not often happen at actuality, in this case, this paper will ignore the bolt thread modeling process, while the "*Binding*" constraints in ABAQUS are used to simulate the contact condition between the thread and the nut. Simultaneously, the number of nuts was increased to avoid the occurrence of the thread failure mode during experiments.

The impact failure process was simulated by the "dynamic, explicit" solver in ABAQUS/Explicit, and the time step was set as 0.012 s according to the measured data collected in the experiments. The ductile metal shear damage constitutive model in ABAQUS is used to simulate the failure process of the structure, and the model parameters are presented in Table 2.

According to the calculation results of the finite element model, the failure process of the connection structure, the effect of the failure, and the safety of the fixed boundary are investigated before carrying out these experiments. It is determined that the experiments are loaded from the height of 2 m with the drop hammer of 270 kg limited by the existing experimental conditions in the laboratory. The two groups of fastening bolts of 12 × M8 and 12 × M10 set up on the fixed boundary, respectively, were adopted to guarantee the complete clamping effect of the tooling boundary.

3. Experimental Results

3.1. Impact Loading. The instantaneous impact velocity of the hammer head in the experiments has been recorded by

Table 2: The material parameters in the FEM.

Material name	Density (ρ)	Young's modulus (E)	Poison ratio	Plastic stress (MPa)	Plastic strain	Fracture strain	Revolution displacement
Aluminum alloy	2.7E-9	70000	0.3	300 370	0 0.05	0.05	1.0
Grade 8.8 high strength bolt	7.89E-9	70000	0.3	680 800	0 0.3	0.3	0.5
Grade 12.9 high strength bolt	7.89E-9	70000	0.3	1080 1200	0 0.3	0.3	0.5
45# iron	7.9E-9	210000	0.3	355 600	0 0.1	0.1	1.0
Shear pin	7.89E-9	211000	0.3	1256 1560	0 0.1	0.1	1.0

the photoelectric velocity measuring devices as shown in Table 3. The hammer impact process was simulated in the form of the initial velocity field in the simulation model, and the impact velocity of the hammer head is calculated by $mgh = (1/2)mv^2$ according to gravity acceleration $g = 9.8\,(\mathrm{m/s^2})$ as shown in Table 3. The time history curve of the drop hammer impact force was collected by the force sensor, as presented in Figure 7.

It indicated that the designed impact velocity is in good agreement with the measured one concluded from the comparison of the impact velocity between the experiment and simulation, and the maximum error is only 1.18%. The time history curves of impact force in experiments are all approximately triangular pulses, and the pulse width is about 2 ms, substantiating that the impact failure experiment of the drop hammer can satisfy the experimental background requirements of the impact loading in the millisecond magnitude.

3.2. Failure Process. In the process of the experiments, the drop hammer falls and simultaneously triggers the high-speed camera switch, when recording the impact failure process. The failure process and results of the experiments are, respectively, shown in Figures 8 and 9. Besides, the comparison between the experiments and simulation results is also made.

The failure process proves that the bolt group in the connection structure is characterized by sequential failure under transverse impact load, the connection interface opens from the pulled side to the pressure side, and the bolts begin to fracture in sequence from the upper side of the bolt group distribution plane. The experimental results shown in Figure 10 demonstrate that the failure position is the bolt group of the connection structure concerned by the experimental design. In addition, all the bolts in the bolt group failed to fracture at the middle surface between the thread and the nut where strength is weaker. Due to the "leverage effect" of the flange, the screw is obviously bent and deformed. Besides, the actual failure mode is the flexural and tensile coupling failure, and there is a sketch shown in Figure 11 of the inner force in the bolts related to the "leverage effect" of the flange and the direction of the slotted displacement marked as ΔL.

Table 3: The instantaneous impact velocity of the hammer head.

Experimental grouping identifier	T-1	T-2	T-3	T-4
Velocity in experiment (m/s)	6.3130	6.2384	6.1882	6.2539
Velocity in FEM (m/s)	6.2610	6.2610	6.2610	6.2610

The experimental results of the shear pins are illustrated in Figure 12, demonstrating that the magnitude shear force is applied to the pin, especially in the no. 4, no. 5, and no. 6 pin which show previous plastic deformation. Additionally, there is no obvious indentation or deformation in the cushion block as shown in Figure 13, no deformation or looseness in the tooling boundary, and no deformation or crack in the flange. In the simulation, the bolts group was also characterized by sequential failure, and there exists no obvious deformation and looseness in the tooling boundary and flange, and the screw has obvious bending deformation. Thus, the simulation model shows the similar failure process as the actual experiments.

4. Analysis of Experimental Results

In the experiments, the response data of bolts force (the data of the no. 5 bolt was not collected in experiment T-4 for limitation of the data acquisition channel) and strain response data of the middle points on the outer surface of the column segment (the strain response signal in the experiment T-4 was not collected for limitation of the data acquisition channel) were collected, respectively. Especially, the initial value of the response curve is the bolt pretightening force, and it was applied manually through the torque wrench. Therefore, the pretightening forces of different bolts are different.

4.1. The Response Data of the Bolts Force. In the experiment T-1, it could be indicated that the bolt group presents a sequential failure characteristic, and the bolts are loaded and then fractured from the tensile side to the compression side of the connecting interface in turn, as shown in Figure 14(a). Otherwise, the distribution characteristic of the bolt group is different on the left and right semicircles. The no. 2, no. 3, and no. 4 bolts in the right semicircle are distributed more intensively, while the no. 6, no. 7, and no. 8 bolts in the left semicircle are distributed more sparsely.

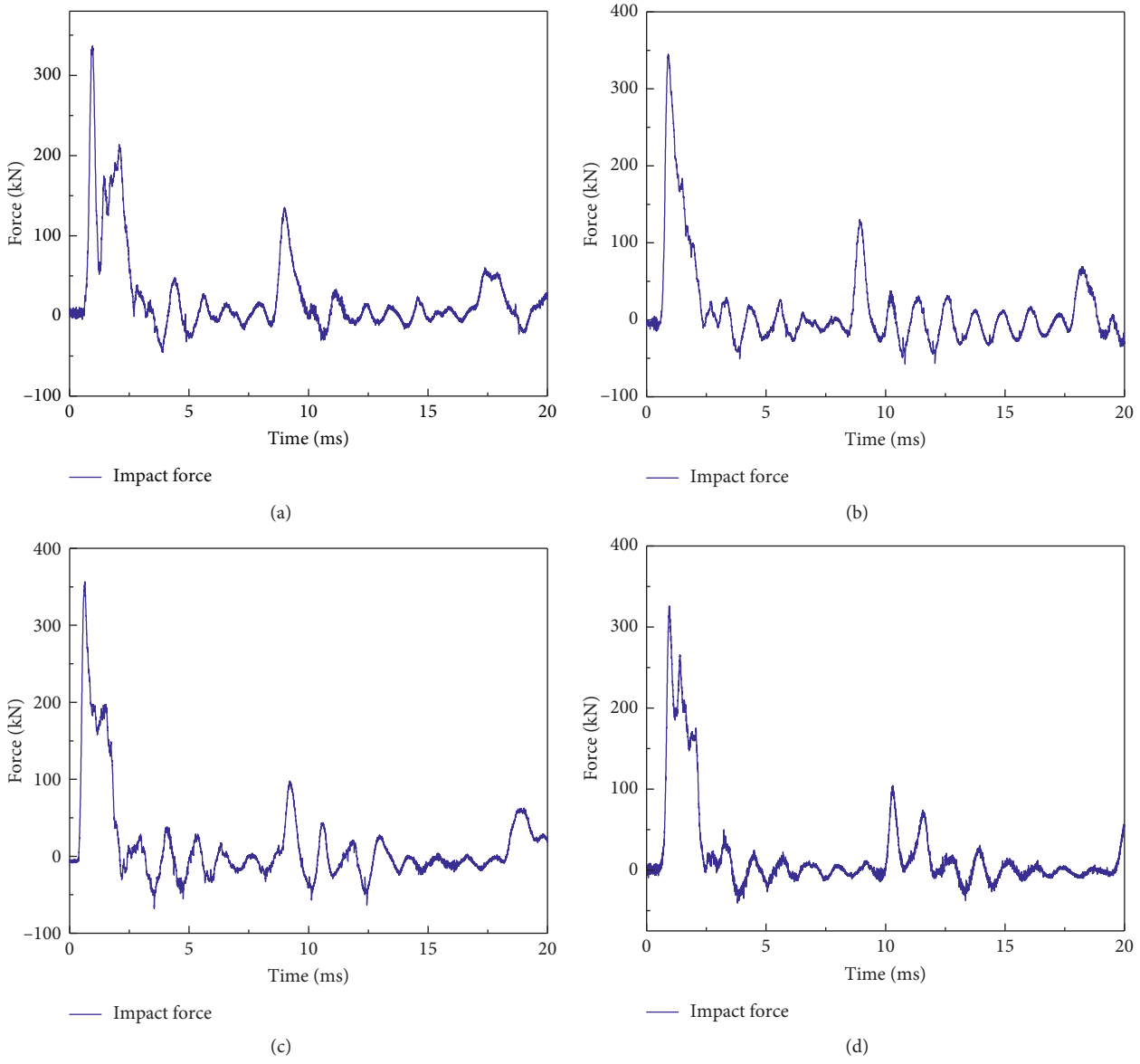

Figure 7: The curves of the impact force. (a) T-1, (b) T-2, (c) T-3, and (d) T-4.

The no. 1 bolt is loaded and fractured at first, with a time range of about 5 ms. The no. 8 Bolt is located on the upper side of the distribution plane, and fracture is almost simultaneous with the no. 1 bolt, followed by no. 2 and no. 7 bolts. It should be noted that the no. 7 bolt and no. 3 bolts are symmetrical to the distribution plane of the bolt group, but the no. 7 bolt is loaded and fractured before no. 3 bolt due to the load bearing of the no. 2 bolt previously. As the distribution condition of no. 2, no. 3, and no. 4 bolts is relatively concentrated and increases the local load bearing capacity, the local deformation of the flange in the loading process is larger, and the bolt force response time is longer than other bolts. The no. 5 bolt did not break at last for the limitation of the pedestal, and the failure duration of the whole bolt group is about 20 ms. Therefore, it can be demonstrated from the experimental phenomena that small deformation appears at the local flange in the topside of the bolt distribution plane for the fast velocity and high amplitude of the impact load and propagation characteristics of the stress wave in the process of impact loading. Additionally, the brittle fracture effect of the corresponding bolts is more obvious.

In the experiment T-2, the bolt group consisted of 12 bolts which were distributed uniformly, and the diameter is M5. The bolt group in this experiment showed the sequential failure characteristic under transverse impact load, and the overall failure duration time of the bolt group was about 20 ms which is similar to the results of the experiments T-1. The no. 7 bolt did not fracture during impact loading due to the limitation of the pedestal. The first five bolts on the upper side of the bolt distribution plane are the initial load bearing and fracture bolts with a failure duration of about 5 ms and the force response peak at about 15 kN. Regarding the lower overall strength of the bolt

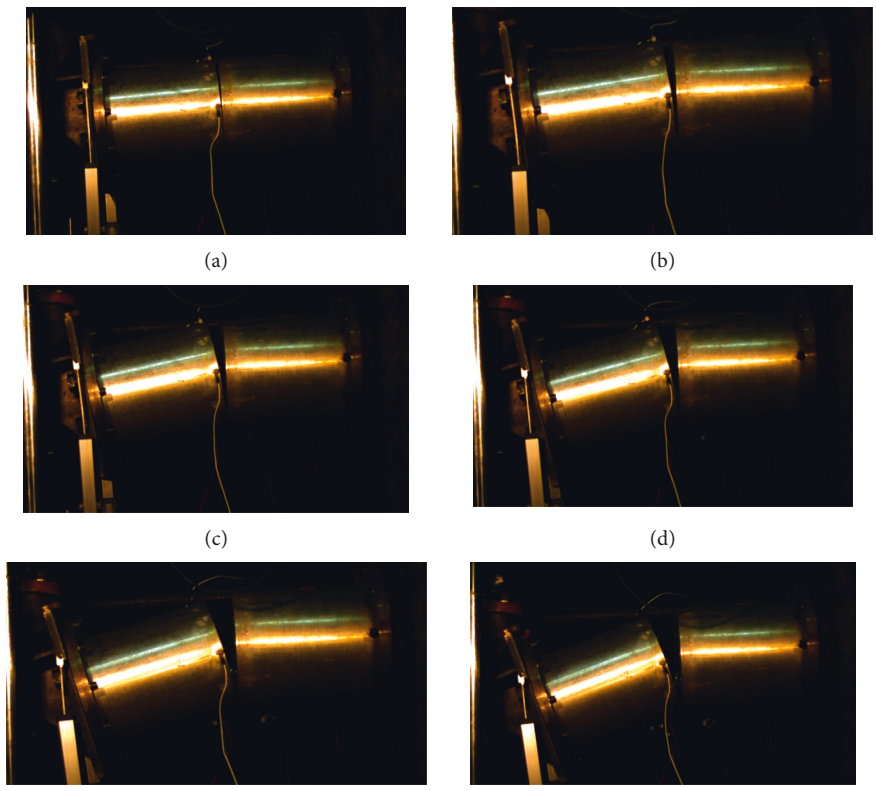

Figure 8: The failure process in the experiments. (a) 0 ms, (b) 5 ms, (c) 10 ms, (d) 15 ms, (e) 20 ms, and (f) 25 ms.

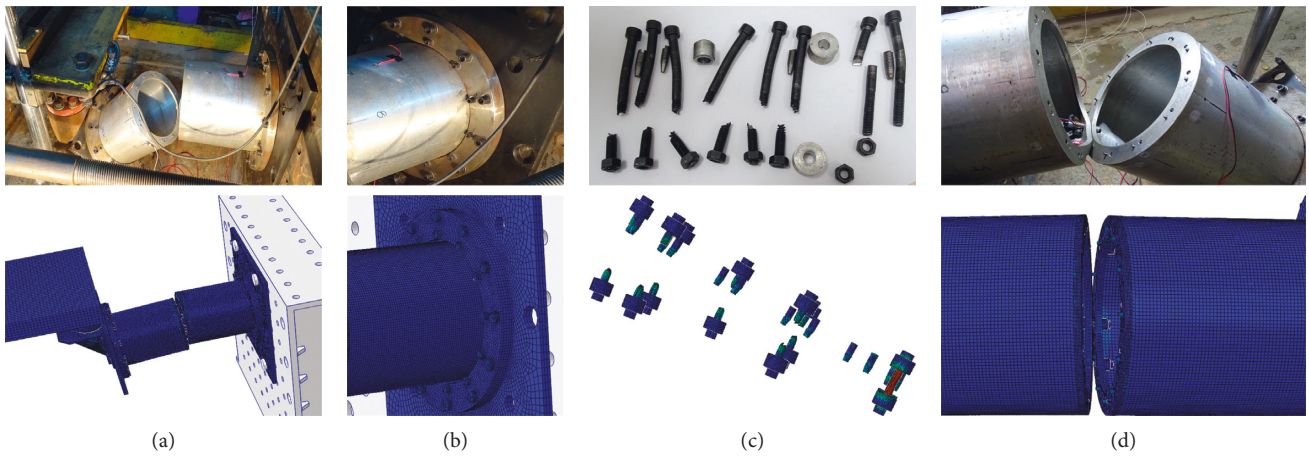

Figure 9: The comparison of the failure results. (a) Overall effect. (b) Boundary. (c) Bolt and pin. (d) Flange interface.

Figure 10: The experimental results of the bolts.

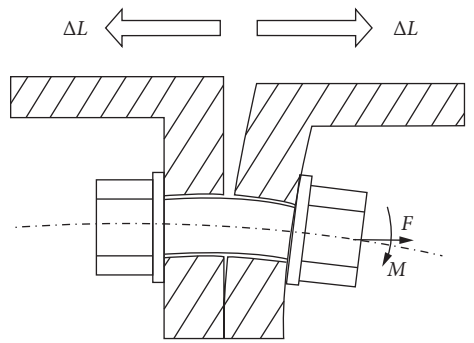

Figure 11: The sketch of the inner force in the bolts.

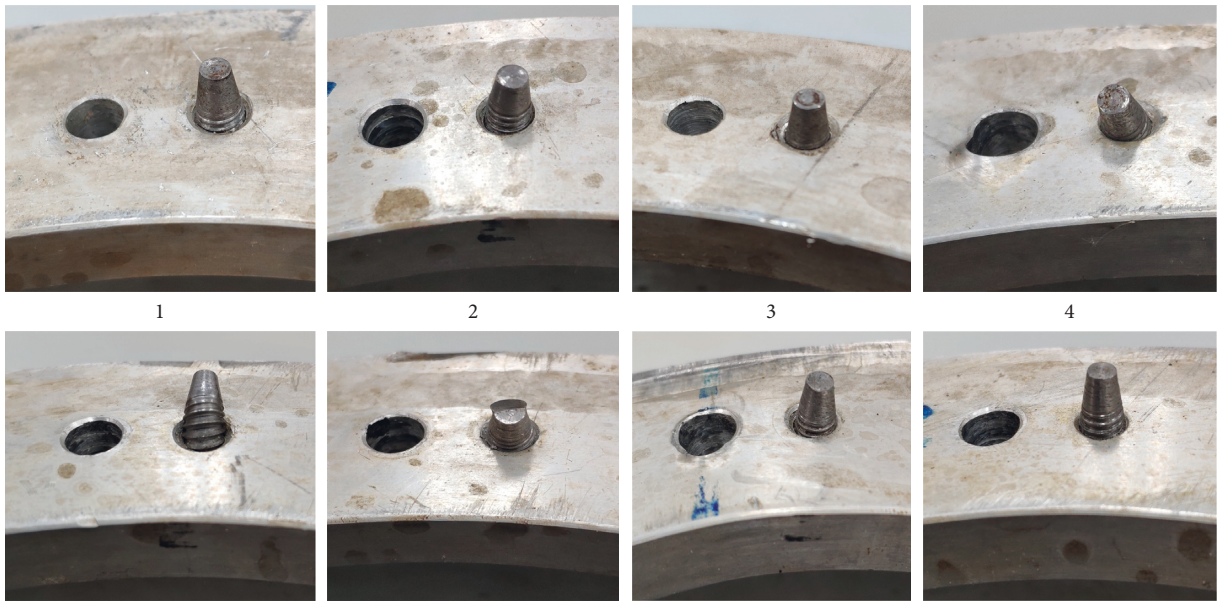

Figure 12: The experimental results of the shear pins.

Figure 13: The experimental results of the cushion block.

group and strong impact load in this experiment, the stress wave propagated in the structure which vibrated in the collision process of the drop hammer, and the obvious fluctuation characteristic is shown in the bolt response curves. The experimental results prove that shear pins and pin holes are featured with obvious extrusion deformation. It was noted that the bolt and shear pins bear large shear action in this experiment, which is the reason for the loosening of the bolt's initial pretightening force presented in the response curves of the bolt force.

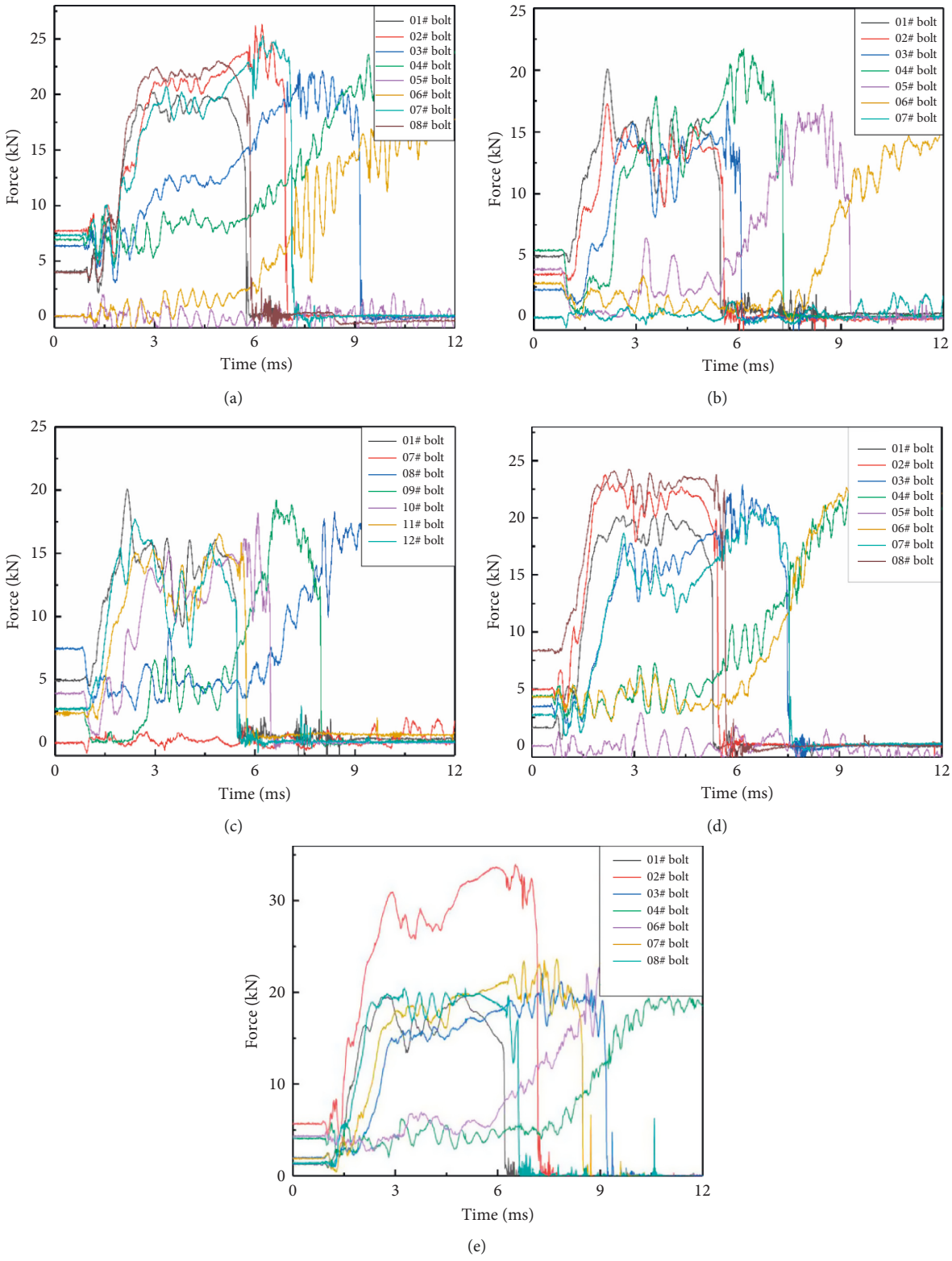

Figure 14: The response curves of the bolts force (experiment). (a) T-1, (b) T-2(1), (c) T-2(2), (d) T-3, and (e) T-4.

In the experiment T-3, there was a 3 mm gap between the bolt and the bolt hole compared with the previous two experiments (T-1 and T-2). The duration time of initial load bearing and fracture bolts in the bolt group is about 5 ms, and the overall failure duration of the bolt group is about 20 ms. The initial load bearing bolts are the no. 1, no. 2, and

no. 8 bolts on the upper side of the bolt group distribution plane. Due to the large pretightening force applied to the no. 2 and no. 8 bolts, the local load bearing capacity is increased, and the response time of these bolts is longer than that of the no. 1 bolt during impact loading. During this experiment, the bolt force response showed the obvious symmetric characteristic, while, at the same time, the no. 2 and no. 8 bolts, no. 3 and no. 7 bolts, and no. 4 and no. 6 bolts were almost loaded and fractured, respectively.

In the experiment T-4, there was a 4 mm gap between the bolt and the bolt hole. The designed sensor (mentioned in Section 2.3) is adopted to collect the bolt response signal, which is also directly collected by applying the strain gauge on the bolt screw. In the bolts group, a 12.9 grade high strength bolt was introduced into the position of the no. 2 bolt to compare and analyze its influence on the response characteristics of the bolt group in the process of impact loading. The bolt force response curve of this experiment shows that no. 1, no. 2, and no. 8 bolts are loaded firstly, and the duration time from load bearing to fracture is about 5 ms. Due to the high strength of the no. 2 bolt and the relatively larger deformation of the connecting local position in the flange corresponding to it, this bolt has a longer response time of about 6.5 ms. The symmetry of the bolt group response on the time scale disappeared, and the response of the left semicircle bolt was significantly advanced. The experimental results prove that the screw has the large bending deformation, because the gap between the bolt and the bolt hole provides the space for staggered extrusion, and the fracture position of the bolt is still the interface between the screw and the nut where strength is weak.

4.2. The Strain Response on the Column Segment. In Figure 15, the time history response curves of strain on the column segment in experiments are, respectively, shown. The signal was collected by applying strain gauges, and it was mainly located on the outside surface of the middle part on the column segment. Limited by the number of signal acquisition channels, the quantity of signals collected by each experiment shows slightly difference.

In these experiments, the bonding position of the strain gauge is the upper surface (the tensile side) and the lower surface (the compression side) of the column segment which installed horizontally. No. 1 and no. 2 strain gauges are applied on the upper surface of the column segment, located at the middle point of the free end and the middle point of the clamped end, respectively; no. 3 and no. 4 strain gauges are applied on the lower surface of the column segment, located at the middle point of the free end and the middle point of the clamped end, respectively (in experiment T-2, no. 4 strain response data were not collected).

According to the strain response curves, on the upper surface of the column segment, the response of the free end (no. 1 strain gauge) precedes that of the clamped end (no. 2 strain gauge), and the amplitude of the latter is about twice that of the former. The response on the upper surface of the column segment is concentrated on the duration time from 1 ms to 6 ms, which corresponds to the time range of the first three bolt failures on the upper side of the bolt group distribution plane. On the lower surface of the column segment, the response of the clamped end (no. 4 strain gauge) precedes that of the free end (no. 3 strain gauge). Additionally, the response amplitude is significantly greater than that of the free end (no. 3 strain gauge). In addition to that, the response amplitude on the lower surface is significantly greater than that on the upper surface of the column segment. In particular, in the experiment T-2, due to the low strength of the bolt group, the strain response time range of the column segment is shorter, and the response amplitude is relatively weakened.

4.3. Comparison of Signal Acquisition Methods. It is difficult to collect the response signals by applying strain gauges directly on the screw for the coherent structural characteristics of the bolted flange connection structure. To solve this problem, the bolt force signal acquisition sensor was designed and fabricated, as described in Section 2.2. In the experiment T-4, the strain gauge was applied on the screw, and the sensors were set up to collect the bolt force response signal at the same time to compare the signal acquisition quality of different measurement methods. In the actual process of this experiment, as there is only 4 mm gap between the screw and the bolt hole, the wires which led to transmit electric signals of strain gauges were extruded and pulled apart during loading, and only the strain gauge on the no. 6 bolt has successfully collected signals. The comparison curve of the signals collected by the strain gauge and the sensor is shown in Figure 16.

Based on the figure, the signal collected by the strain gauge directly applied on the screw is basically the same as that collected by the sensor in the response duration time (about 9 ms when the bolt began to respond and about 21 ms when the bolt failed). In the response amplitude, the signal curve of the sensor is smoother. The response peak measured by the strain gauge applied on the screw is slightly higher than that measured by the sensor, which may be related to the strain gauge bonding position on the screw. Since the strain gauge of the sensor is applied on the outside surface of the bearing steel sleeve and the bearing steel is always within the elastic range during loading, the response signal will return to zero after the bolt fractures. However, there is residual deformation in the bonding position of the strain gauge applied on the screw, so the response signal fails to return to zero. To conclude, the signal quality of bolt force response collected by the sensor is higher and more stable, and the actual response characteristics of the bolt force can be collected well by this method.

4.4. Results of FEM. In order to verify the numerical simulation accuracy, the corresponding finite element model is established according to Section 2.3. The response data of bolts force are the key data for reflecting the

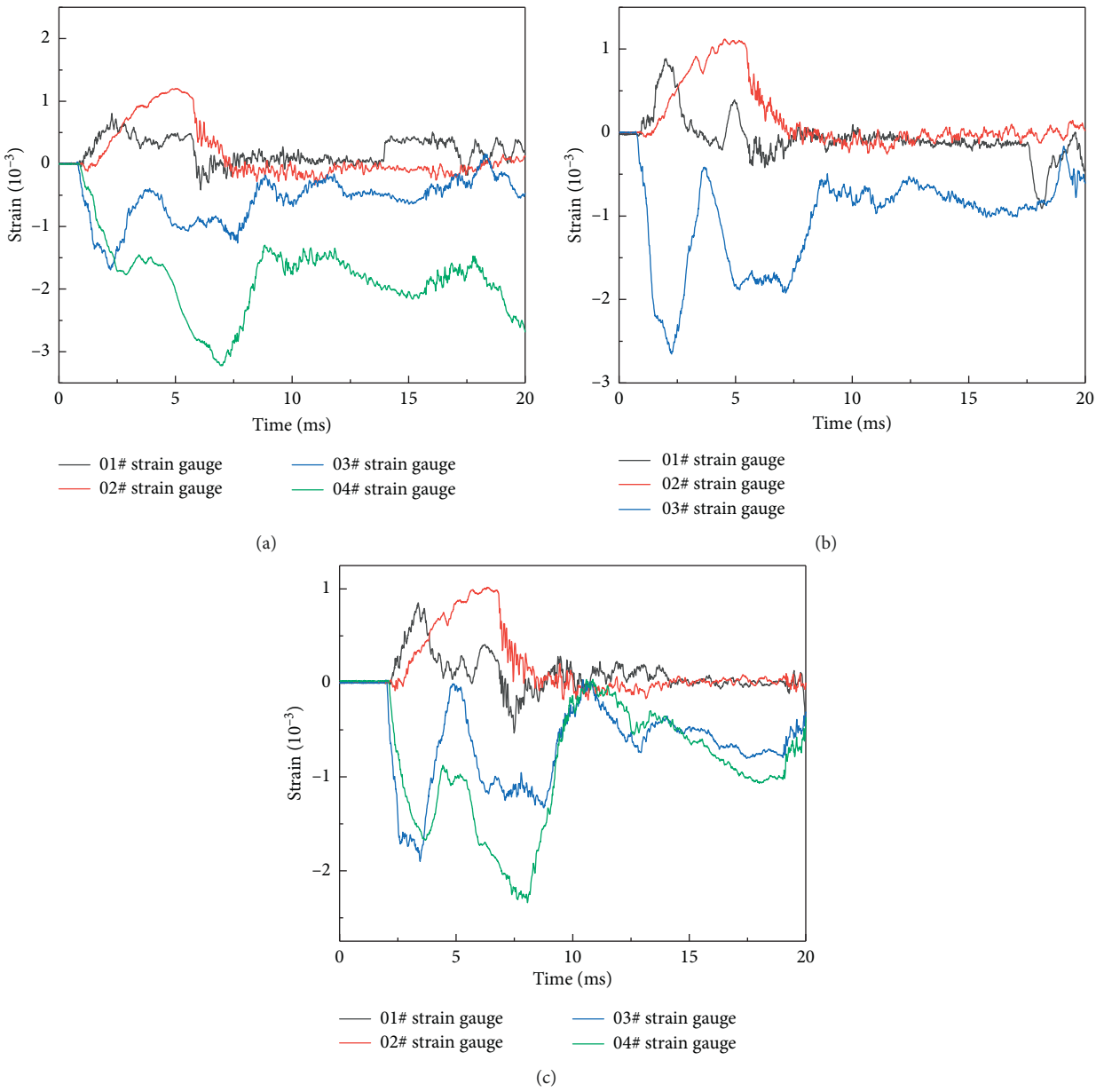

Figure 15: The strain response curves of the middle points on the outer surface of the column segment. (a) T-1, (b) T-2, and (c) T-3.

response mechanism of the connection structure under transverse impact load. As shown in Figure 17, the response results of bolt force in the finite element models corresponding to the experiments are, respectively, output. The pretightening force of the bolts collected from the experiments which also applied to the simulation model can be found in Table 4.

With the bolt force response curve of simulation model T-1 as an example, the response amplitude of the single bolt in the bolt group is around 20 kN, the bolt response amplitude measured in the experiment is about 21 kN, and the error between them is about 5%. The response time range of the initial load bearing bolt (no. 1) is about 3 ms, the actual measurement is about 3.5 ms, and the error is about 16.67%. The comparison results show that the experimental and simulation results are in good agreement with each other in the amplitude of bolt force response. In the simulation, the stress response data at the integral point of the outermost element of the bolt's middle surface which first deleted were output, and then they were converted into the force response of the bolt. Therefore, compared with the experimental data, the fracture failure of the bolts presents faster. The bolt force response sensor used in the experiment can mainly collect the axial force response signal, which is designed by applying the strain gauge on the bearing steel sleeves. Practically, the failure mode of bolts on the upper side of the bolt group is mainly the flexural and tensile coupling failure, while the lower side bolts bear magnitude shear loading. Therefore, the experimental response collected by the designed sensor fails to fully reflect the complex stress state of bolts in the lower

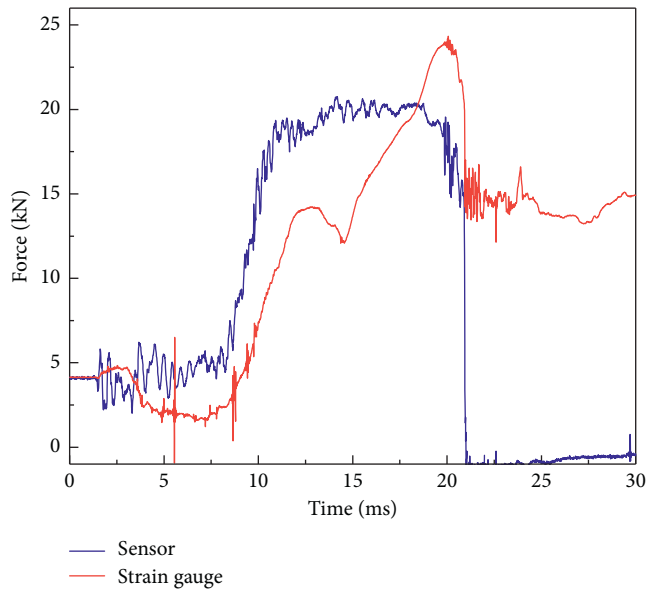

Figure 16: The comparison of the strain gauge and the sensor signal.

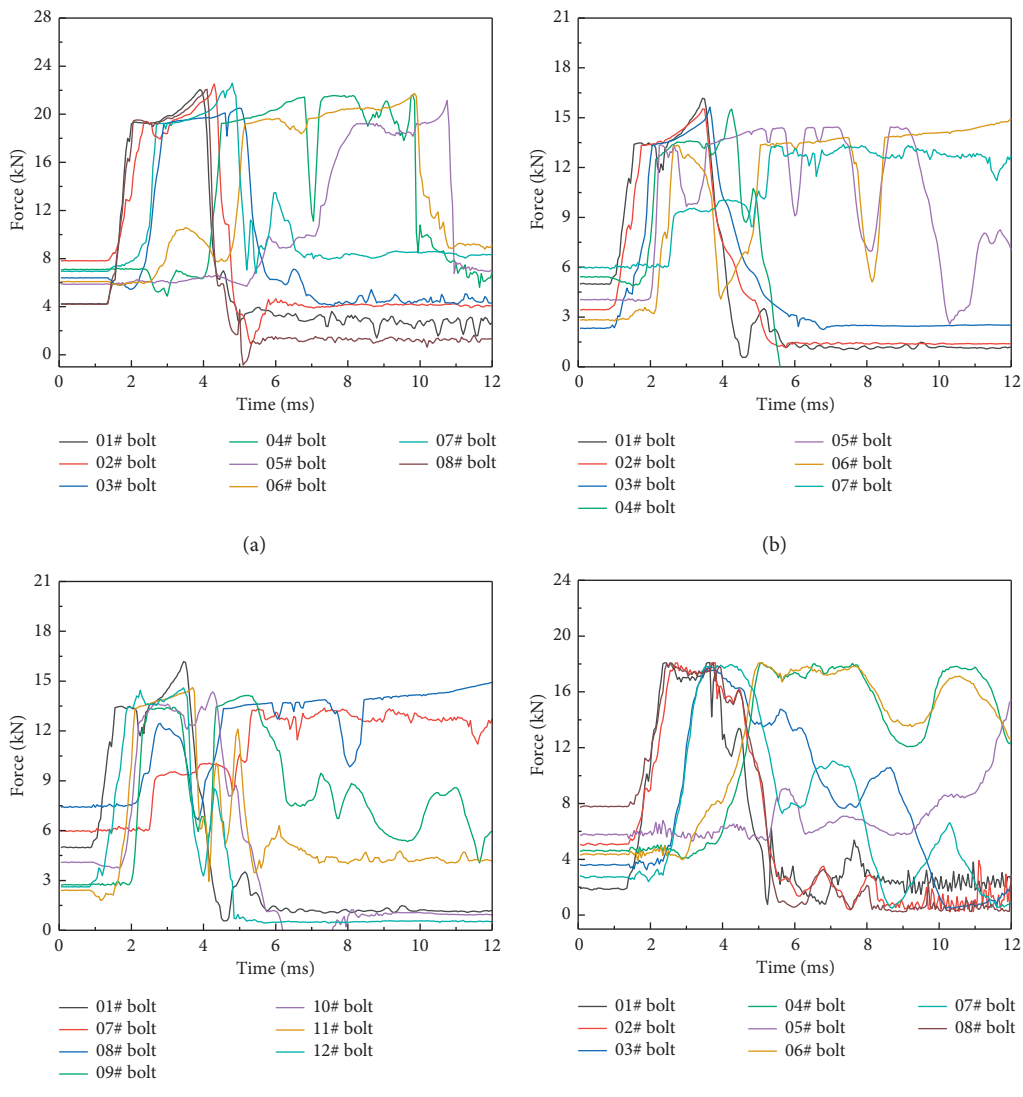

Figure 17: Continued.

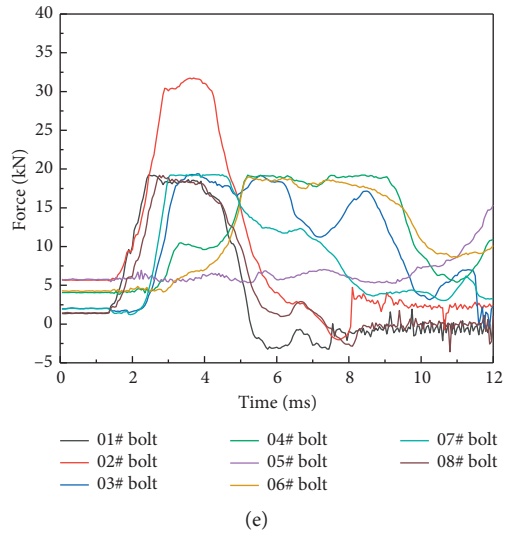

(e)

Figure 17: The response curves of the bolts force (simulation). (a) T-1, (b) T-2(1), (c) T-2(2), (d) T-3, and (e) T-4.

Table 4: The pretightening forces of the bolts in the experiments (kN).

Identifier (experiment)	01# bolt	02# bolt	03# bolt	04# bolt	05# bolt	06# bolt	07# bolt	08# bolt	09# bolt	10# bolt	11# bolt	12# bolt
T-1	4.0643	7.7225	6.3708	6.9256	—	—	7.3243	3.9776				
T-2	4.9398	3.5032	2.2526	5.4375	3.9079	2.7682	—	7.4460	2.6895	3.9207	2.3218	2.7055
T-3	1.5986	4.9488	3.4702	4.3534	—	4.2980	2.7414	8.3778				
T-4	1.2667	4.3405	1.9882	4.0957	—	5.6680	1.9132	1.3920				

side, which is also a reason for the error between experimental and simulation results. However, as mentioned above, the three initial load bearing bolts determine the load bearing capacity of the whole connection structure. In engineering practice, it can be considered that the failure of the initial load bearing bolts means the failure of the whole connection structure, and it is assumed that the simulation model can reflect the loading capacity of the initial load bearing bolts well. In other words, it can also simulate the working capacity of the whole connection structure well. In particular, a grade 12.9 high strength bolt was introduced into experiment T-4, and the characteristics of the higher response amplitude and longer response duration time were tested. In this case, it can be well embodied in the simulation (Figure 17(e)).

What needs illustration is that the pretightening force of some bolts was not collected during the experiments as shown in Table 4. According to the mechanical design standard, the corresponding bolts were applied to 6 kN pretightening force in the simulation model.

In the course of the experiments, the resistance-type displacement sensor was set to collect the response data of the slotted displacement of the connecting interface, and the installation position is shown in Figure 4. The comparison between the experimental results and the simulation model is taken as presented in Figure 18 indicating that the simulation results have high precision, and the maximum error is less than 10%. In conclusion, in practical design and engineering application, it can be considered that the conclusion calculated by the FEM is reliable.

5. Conclusion

In the proposed study, based on the experimental specimens simplified from the bolted flange connection structure between stages of missiles, four impact failure experiments were designed and carried out, and the FEM corresponding to the experiments was established. Then, the following conclusions could be obtained:

(1) The experimental results showed that the failure characteristic of the bolt group is sequential failure, and the failure characteristic of the single bolt in the bolt group is coupled flexural-shear failure due to the "leverage effect" of the flange.

(2) Through comparing the response time history curves of bolt force, it can be found that that the first three bolts in the upside of the bolt distribution plane are the initial load bearing bolts, and the load bearing capacity of connection structure is determined. It is explained that the greater the pretightening force and the density of bolt distribution are, the larger the local load bearing and the deformation of the local flange under impact load are.

(3) To collect the force response data of a single bolt, a response signal acquisition sensor of the bolt force

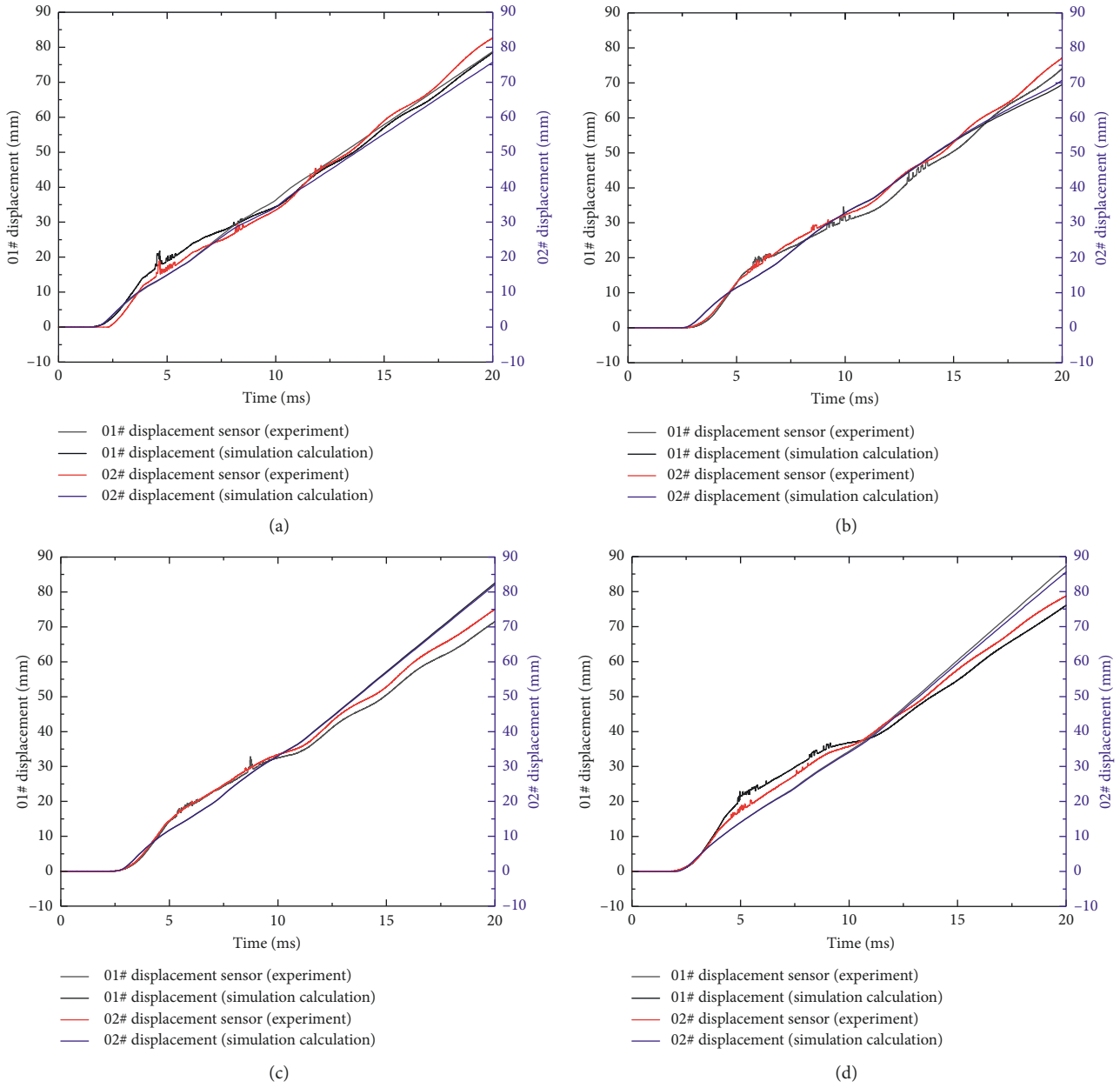

Figure 18: The comparison of the slotted displacements. (a) T-1, (b) T-2, (c) T-3, and (d) T-4.

is designed using the bearing steel sleeve. Compared with the signal acquisition method of applying strain gauges directly on the screw, the signal acquisition of the sensor is stable; the quality is better, and it can reflect the response characteristics of a single bolt well.

(4) It can be demonstrated that the simulation data of the bolts force calculated by the FEM possesses good precision compared with the measured data, and the failure mechanism simulated by the FEM coincides well with the actual condition. As a result, the conclusion calculated by the FEM can be regarded as reliable instruction in actual engineering design and application.

Data Availability

The data used to support the findings of this study are available from the corresponding author upon request.

Conflicts of Interest

The authors declare that there are no conflicts of interest regarding the publication of this paper.

Acknowledgments

This study was sponsored by the open fund of National Key Laboratory of Science and Technology on Vacuum

Technology and Physics of CAST (no. ZWK1702), Chinese National Natural Science Foundation (no. 51605483), and National Key Research and Development Program (no. 2017YFB1300900).

References

[1] L. Gaul and J. Lenz, "Nonlinear dynamics of structures assembled by bolted joints," *Acta Mechanica*, vol. 125, no. 1–4, pp. 169–181, 1997.

[2] I. R. Grosse and L. D. Mitchell, "Nonlinear axial stiffness characteristics of bolted joints," *Journal of Mechanical Design*, vol. 122, no. 3, pp. 442–449, 1990.

[3] I.-S. Chang, "Investigation of space launch vehicle catastrophic failures," *Journal of Spacecraft and Rockets*, vol. 33, no. 2, pp. 198–205, 1996.

[4] J. L. Otegui, P. G. Fazzini, and A. Marquez, "Common root causes of recent failures of flanges in pressure vessels subjected to dynamic loads," *Engineering Failure analysis*, vol. 16, no. 6, pp. 1825–1836, 2009.

[5] S. Daouk, F. Louf, C. Cluzel et al., "Study of the dynamic behavior of a bolted joint under heavy loadings," *Journal of Sound and Vibration*, vol. 392, pp. 307–324, 2017.

[6] J. D. Reid and N. R. Hiser, "Detailed modeling of bolted joints with slippage," *Finite Elements in Analysis and Design*, vol. 41, no. 6, pp. 547–562, 2005.

[7] R. A. Ibrahim and C. L. Pettit, "Uncertainties and dynamic problems of bolted joints and other fasteners," *Journal of Sound and Vibration*, vol. 279, no. 3–5, pp. 857–936, 2005.

[8] Z.-Y. Qin, Q.-K. Han, and F.-L. Chu, "Analytical model of bolted disk-drum joints and its application to dynamic analysis of jointed rotor," *Proceedings of the Institution of Mechanical Engineers, Part C: Journal of Mechanical Engineering Science*, vol. 228, no. 4, pp. 646–663, 2014.

[9] H. Van-Long, J. Jean-Pierre, and D. Jean-François, "Behaviour of bolted flange joints in tubular structures under monotonic, repeated and fatigue loadings I: experimental tests," *Journal of Constructional Steel Research*, vol. 85, pp. 1–11, 2013.

[10] G. S. Prinz, A. Nussbaumer, L. Borges, and S. Khadka, "Experimental testing and simulation of bolted beam-column connections having thick extended endplates and multiple bolts per row," *Engineering Structures*, vol. 59, pp. 434–447, 2014.

[11] Y. Guo, Y. Wei, Z. Yang, C. Huang, X. Wu, and Q. Yin, "Nonlinearity of interfaces and force transmission of bolted flange joints under impact loading," *International Journal of Impact Engineering*, vol. 109, pp. 214–223, 2017.

[12] J. Kim, J.-C. Yoon, and B.-S. Kang, "Finite element analysis and modeling of structure with bolted joints," *Applied Mathematical Modelling*, vol. 31, no. 5, pp. 895–911, 2007.

[13] Y. Luan, Z. .–Q. Guan, G.-D. Cheng, and S. Liu, "A simplified nonlinear dynamic model for the analysis of pipe structures with bolted flange joints," *Journal of Sound and Vibration*, vol. 331, no. 2, pp. 325–344, 2012.

[14] X. Lu, Y. Zeng, Y. Chen, X.-F. Xie, and Z. Guan, "Transient response characteristics of a bolted flange connection structure with shear pin/cone," *Journal of Sound and Vibration*, vol. 395, pp. 240–257, 2017.

[15] P. Schaumann and M. Seidel, "Failure analysis of bolted steel flange," in *Proceedings of the seventh International Symposium on Structural Failure and Plasticity (IMPLAST2000)*, Melbourne, Australia, October 2000.

[16] M. Abid, A. Khan, D. H. Nash, M. Hussain, and H. Abdul Wajid, "Optimizad bolt tightening strategies for gasketed flanged of different size," *International Journal of Pressure Vessels and Piping*, vol. 139-140, pp. 22–27, 2016.

[17] M. Abid and D. H. Nash, "A parametric study of metal-to-metal contact flanges with optimized geometry for safe stress and no-leak conditions," *International Journal of Pressure Vessels and Piping*, vol. 81, no. 1, pp. 67–74, 2004.

[18] B. Bartlomiej and G. Witold, "Effect of damaged circle flange-bolted connections on behaviour of tall towers, modelled by multilevel substructuring," *Engineering Structures*, vol. 111, pp. 93–103, 2016.

[19] Y. Chen, Q. Gao, and Z.-Q. Guan, "Self-Loosening failure analysis of bolt joints under vibration considering the tightening process," *Shock and Vibration*, vol. 2017, Article ID 2038421, 15 pages, 2017.

[20] J. G. Williams, R. E. Anley, D. H. Nash, and T. G. F. Gray, "Analysis of externally loaded bolted joints: Analytical, computational and experimental study," *International Journal of Pressure Vessels and Piping*, vol. 86, no. 7, pp. 420–427, 2009.